problem with single-phase melting simulations is the possible superheating of the solid during heating and undercooling of the liquid during cooling due to the kinetics [22] especially at high pressure, which could be reduced by two-phase simulation [23]. The two-phase simulation was conducted by constructing a solid–liquid model by combining the solid and liquid models at the same pressure and temperature from the single-phase simulation. Figure 6 shows the simulation results along with former studies on stishovite melting. At 20 GPa, single-phase simulation appears to be closer to experimental data than the two-phase simulation, possibly due to the simplicity of the force field or the interface effect that is more pronounced at low pressure [14]. At high pressures, the two-phase simulation yielded more accurate results. The melting curve of stishovite is obtained from MD simulation results along with experimental data. The slope of the proposed melting curve is consistent with that computed from single-phase simulation. The MD simulation results are close to the static DAC results at low pressure, and shock wave data at high pressure. This appears to validate the interpretation of superheating of the solid along fused quartz and quartz Hugoniots by Lyzenga et al. [15]. With the melting curve of stishovite constrained, the silica phase diagram is extended to the megabar regime.

4. Conclusion

In conclusion, the Hugoniot of stishovite up to 235 GPa was obtained by shocking pure stishovite samples synthesized from a multi-anvil high-pressure press. The coesite Hugoniot in the stishovite regime is in agreement with former study and extended to 140 GPa. Hugoniots centered at various silica polymorphs have been obtained, from which the Grüneisen parameter for stishovite under compression is experimentally determined. The new molecular dynamics modeling validates the interpretation of shock melting experiments on fused quartz and quartz, and the phase diagram of silica is extended to the megabar regime with a sound experimental and theoretical basis.

References

1. Hemley R J, Prewitt C T, Kingma K *Rev. Mineral.* **29** 41 (1994)
2. Knittle E, Jeanloz R *Science* **251** 1438 (1991)
3. Song X, Ahrens T J *Geophys. Res. Lett.* **21** 153 (1994)
4. Chao E C T et al. *J. Geophys. Res.* **67** 419 (1962)
5. El Goresy A et al. *Science* **288** 1632 (2000)
6. McQueen R G, Fritz J N, Marsh S P *J. Geophys. Res.* **68** 2319 (1963)
7. Wackerle J *J. Appl. Phys.* **33** 922 (1962)
8. Fowles R *J. Geophys. Res.* **72** 5729 (1970)
9. Ahrens T J, Rosenberg J T, in *Shock Metamorphism of Natural Materials* (Eds B M French, N M Short) (Baltimore: Mono Book Corp., 1968) p. 59
10. Trunin R F *Shock Compression of Condensed Materials* (Cambridge: Cambridge Univ. Press, 1998)
11. Podurets M A et al. *Izv. Akad. Nauk SSSR Fiz. Zemli* **17** 9 (1981)
12. Ito E, Furnish M D, Sandia Report SAND-95-2342 (1995)
13. Luo S-N et al. *Geophys. Res. Lett.* (2002), in press
14. Luo S-N et al. *Earth Planet. Sci. Lett.* (2002), in press
15. Lyzenga G A, Ahrens T J, Mitchell A C *J. Geophys. Res.* **88** 2431 (1983)
16. Rubie D C *Phase Transitions* **68** 431 (1999)
17. Ahrens T J, in *High Pressure Shock Compression of Solids* (Eds J R Asay, M Shahinpoor) (New York: Springer-Verlag, 1993) pp. 75–114
18. Cohen R E, Gülseren O, Hemley R J *Am. Mineral.* **85** 338 (2000)
19. Akins J (Private communication)
20. Shen G, Lazor P *J. Geophys. Res.* **100** 17699 (1995)
21. Belonoshko A B, Dubrovinsky L S *Geochim. Cosmochim. Acta* **59** 1883 (1995)
22. Allen M P, Tildesley D J *Computer Simulation of Liquids* (Oxford: Clarendon Press, 1987)
23. Strachan A, Çağin T, Goddard W A III *Phys. Rev. B* **60** 15084 (1999)
24. Hemley R J et al. *Solid State Commun.* **114** 527 (2000)
25. Panero W R, Benedetti L R, Jeanloz R *J. Geophys. Res.* (2001), submitted
26. Marsh S P *LASL Shock Hugoniot Data* (Berkeley: Univ. of California Press, 1980)
27. Al'tshuler L V, Trunin R F, Simakov G V *Izv. Akad. Nauk SSSR Fiz. Zemli* (10) 1 (1965)
28. Watanabe H, in *High-Pressure Research in Geophysics* (Adv. in Earth and Planetary Sci., Vol. 12, Eds S Akimoto, M H Manghnani) (Tokyo: Center for Acad. Publ. Japan, 1982) pp. 441–464
29. Zhang J et al. *J. Geophys. Res.* **98** 19785 (1993)
30. Jackson I *Phys. Earth Planet Int.* **13** 218 (1976)
31. Kanzaki M *J. Am. Ceram. Soc.* **3** 3706 (1990)

Minerals of the deep geospheres

D Yu Pushcharovskiĭ

In this report I discuss the composition and structure of the Earth's mantle. Analysis of seismic tomography maps and the data on the material composition of the mantle shows that the mantle consists of several concentric zones, instead of the commonly accepted two zones, the upper and the lower. As in the Earth's crust, silicates are the predominant substance of the mantle, but structurally the silicates of the mantle differ substantially from those of the crust. More than one hundred tetrahedron complexes in the silicates of the Earth crust are replaced by no more than 20 structure types of this class of minerals in the mantle, and the main difference between these types lies in the transformation of Si tetrahedrons into Si octahedrons. In this sense, one can say that stishovite has opened up a new chapter of the crystal chemistry of silicates. New data on the structural transformations of minerals in the deep geospheres suggest that the mineralogical diversity of the deep zones of the mantle is much poorer than that of the Earth's crust, but nevertheless the mantle mineralogy is not as primitive as it was believed even two to three decades ago.

One of the most intriguing problems of geology in the past decades is related to studies of the composition and structure of the deep geospheres of the Earth. Such research in the Earth sciences is of top priority, since more than 90% of matter in the universe is under pressures greater than 1 GPa. The pressure range in the universe is enormous: pressures vary by more than 60 orders of magnitude. In intergalactic space, there is one atom to more than one cubic centimeter of space, while at the center of neutron stars the state of matter is comparable to the Sun's mass (which is approximately 300 thousand times greater than the Earth's mass) compacted into a volume smaller than that of the Earth (the Earth's volume is approximately one million times smaller than the Sun's).

However, the problem of predicting the state of matter in the deep geospheres is extremely complicated, possibly even more complicated than studies of outer space, since the range of direct data pertaining to the state of matter in the deep zones is extremely limited. In this connection, for a long time the mineral aggregate from a kimberlite pipe in Lesotho, South Africa, occupied the center of the stage. This aggregate is considered as a representative of mantle rock deposited at a depth of roughly 250 km. However, in December 1999, a report appeared about the discovery on Malaita, a volcanic island in the Solomon islands in southwestern Pacific Ocean, of a sample related to the rock of the lower mantle at a depth of 770 km and containing diamond and majorite crystals [1]. The core lifted out of the deepest borehole drilled on Earth on the Kola Peninsula (the depth of the borehole is 12262 m) broadened our scientific ideas about the deep horizons of the Earth's crust. Although this is an outstanding technological achievement, it must be admitted that with respect to the size of the Earth only its top shell has been 'scratched' so far. At the same time, the most recent geophysical data and experimental studies of structural transformations of minerals already make it possible to model many features of the composition and structure of the deep zones of the Earth and the processes taking place in the deepest regions. The knowledge of such processes helps to solve such key issues of modern natural science as the formation and evolution of our planet, the geodynamic stability of the Earth's crust, estimation of the risks involved in burying dangerous waste at

great depths, and the energy resources of the Earth (to name only some such issues).

Figure 1a shows the commonly accepted model of the Earth's interior developed by analyzing the velocity of seismic-wave propagation. The first boundary of this type, separating the Earth's core and the mantle, was established in 1909 by the Croatian seismologist Mohorovichich. In the mid-'50s of the past century two new boundaries were added, one separating the upper and lower mantles and the other separating the outer and inner cores.

Today it is known that many discontinuities in the seismic-wave velocities that have been detected in the deep geospheres correlate with the structural transformations of the mantle minerals (Fig. 2). For instance, the boundary at 410 km is related to the olivine – wadsleyite transformation, and the boundary at 520 km is related to the subsequent transformation of wadsleyite into spinel-like ringwoodite. On the whole, as Fig. 3 shows, the relatively homogeneous concentric zone limited by the depths of 400 and 600 km, primarily contains phases with structures of garnet and spinel type. Below the global boundary at 670 km this association is replaced with perovskite-like phases (which occupy about 70% of the volume of the lower mantle), Mg-wuestite (20%) with a structure of NaCl type, and stishovite, phases considered as a solid solution of corundum and ilmenite and carnegieite $NaAlSiO_4$ which is a structural analog of the Ca-ferrite $CaFe_2O_4$.

Most researchers considered these boundaries at 410, 520, and 670 km as global. The latest seismic tomography data point to new boundaries of this type at depths of 900, 1700, and 2900 km and also to local or intermediate boundaries at 1200 – 1300 and 1900 – 2000 km and some other depths, which makes it possible to revise the commonly accepted model of the structure of deep geospheres in general and the lower mantle in particular. A new model of the Earth's structure has been developed through analysis of the propagation of density inhomogeneities in the mantle revealed by the data from seismic tomography maps for different depth levels and
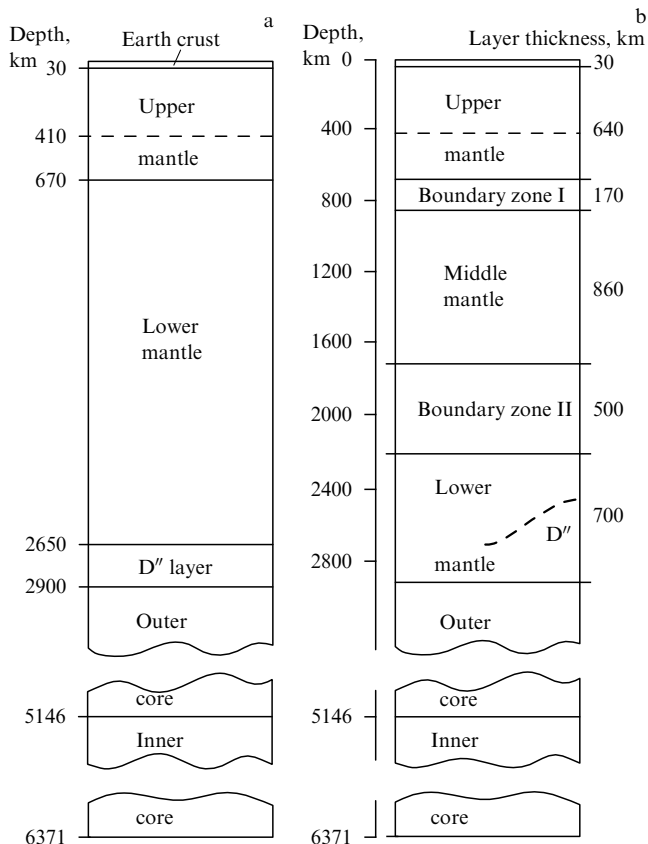

Figure 1. Models of the Earth's structure: (a) the commonly accepted model; (b) a new model based on the analysis of seismic tomography maps and the data on mantle composition and seismic boundaries. Layer thickness may vary by 10%.
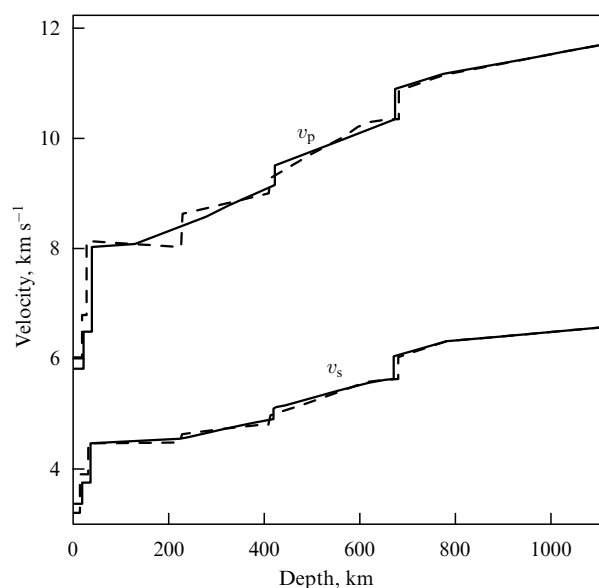

Figure 2. Standard seismic profile characterizing the increase in the velocities of longitudinal (v_p) and transverse (v_s) seismic waves in the deep geospheres.
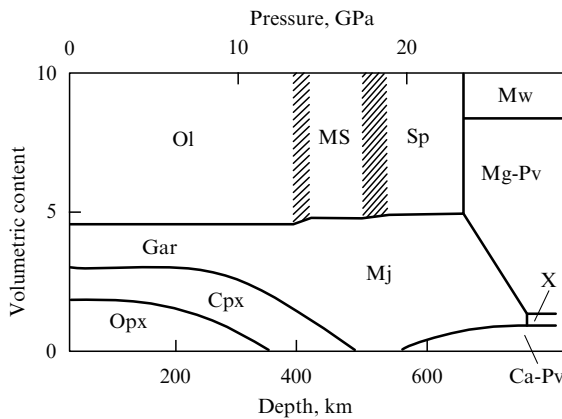
Figure 3. Variation of the volumetric content of the pyrolite minerals with increasing pressure (depth). The symbols of the minerals are as follows: Ol, olivine; Gar, garnet; Cpx, monoclinic pyroxenes; Opx, rhombic pyroxenes; MS, "modified spinel", or wadsleyite; Sp, spinel; Mj, majorite; Mw, magnesio-wuestite; Mg-Pv, Mg-perovskite; Ca-Pv, Ca-perovskite; and X, expected Al-containing phases with structures of the type of ilmenite, Ca-ferrite, and/or hollandite.

through the use of new information about intramantle geophysical boundaries and data on mineral transformations at high pressures [2]. The cornerstone of this new model lies in the recognition of a middle mantle between 840 and 1700 km, which is separated from the upper and lower mantles by boundary zones, 170 and 500 km thick (Fig. 1b). There is also a strong correlation of the boundaries of the new geospheres with the pressures that determine mineral reactions, while the types of structural transformations become more and more diversified as the pressure increases.

Let us examine only the latest data. For instance, the discontinuity in the increase of the seismic-wave velocity at 1200 km is related to the structural transformation of stishovite into a phase with a structure of $CaCl_2$ type, which is a rhombically distorted structural analog of rutile [3], while the phase with spinel composition at such pressures crystallizes in the structure type of calcium titanate. The new data point to the possible replacement at a depth of 1700 km of ion-covalent bonds in a structure of Mg-wuestite with bonds characterized by a metallic type of interatomic interaction [4]. A reaction between iron and corundum, which leads to formation of wuestite and an iron–aluminum alloy, is also possible at this depth [5].

Dubrovinsky et al. [3] have substantiated the disproportioning of Mg-Fe perovskite at a depth of 2000 km, a process accompanied by the formation of Mg-wuestite and silicon oxide whose structure is intermediate between $\alpha\text{-}PbO_2$ and ZrO_2. This phase has recently been detected in shergottites. At the same depth the halite-like form of wuestite is replaced by the nickeline-like form of wuestite [6] and disproportioning of ferripericlase to wuestite and periclase occurs [7]. At even greater pressures the electronic structure of atoms of individual elements may change. For instance, it has been proved that from 2200 km downward (beyond 100 GPa) the iron atoms in pure wuestite may transform from the high-spin state to the low-spin state [8]. Funamori and Jeanloz [9] have also established that at such depths Al_2O_3 with the corundum structure transforms to the rhombic structure of Rh_2O_3, with the molar volume decreasing by 4%. All these results helped in developing the new model of the Earth's structure, in which the lower mantle is

not as homogeneous as assumed earlier. This new model has been gaining support.

Of course, as a general conclusion, it must be admitted that the mineralogical diversity of the deep zones is poorer than that of the Earth's crust. However, the new data suggest that the mantle mineralogy is not as primitive as it was assumed to be only two or three decades ago.

As is known, silicates dominate in the Earth crust: they occupy about 95% of the volume of the continental crust. At the same time, one must bear in mind that the silicates of the Earth's crust comprise only 0.6 mass % of their total content in the Earth [10]. Thus, the main fraction of this class of minerals is concentrated in the mantle. However, structurally the mantle silicates differ dramatically from the silicates of the Earth crust, primarily in that Si tetrahedrons are transformed into Si octahedrons [11]. Presently the stability of silicates with Si tetrahedrons under pressures corresponding to mantle conditions is considered as a unique phenomenon. One of the few examples of this type, $ZrSiO_4$ with the scheelite structure, is characterized by extremely low compressibility and, correspondingly, a large bulk modulus (301.4 GPa) [12], which determines the stability of the structure under the pressures at depths of about 1300 km. The possibility of formation at great depths of mineral phases with Si octahedrons was first corroborated by Stishov and Popova [13] in their study of the structure of stishovite, which in this sense may be considered as the cornerstone of a new chapter in the history of the crystal chemistry of silicates. The subsequent high-pressure experiments conducted by Hazen and Finger [14] revealed that in most rock-forming silicates in the 8–30 GPa pressure range the average Si–O distances in tetrahedrons decrease to the critical value of 1.59 Å and that the SiO_4 tetrahedrons transform into SiO_6 octahedrons. An example of this type of mineral phase is the (Fe, Mg)-perovskite $(Mg_{0.88}Fe_{0.12})SiO_3$ with a framework of Si octahedrons. As shown in Fig. 4, rhombic distortion in this structure type increases with pressure. The number of such mineral phases with SiO_6 octahedrons grows from year to year, and today this family includes more than 30 compounds of 18 structure types, which can be broken down into two groups: (a) those with the joint presence of Si tetrahedrons and Si octahedrons, and (b) those with the presence of only Si octahedrons. Such silicates dominate the mantle down to approximately 2900 km. Speaking of structures with Si octahedrons, it must be noted that the number of structure types inherent in them is seven.
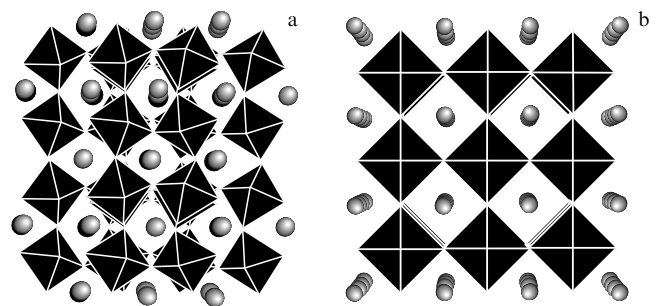

Figure 4. (a) Rhombically distorted structure of (Fe, Mg)-perovskite forming in the lower mantle, and (b) idealized structure of cubic perovskite (according to Ref. [5]).

The oxygen atoms in all such structures are extremely closely packed. Silicates with the structure types of rutile-stishovite, hollandite, and the Ca-ferrite $CaFe_2O_4$ form a single structure-homologous series, in which columns of (Si, Al)-octahedrons coupled along the edges serve as the common structural element (Fig. 5). Phases with a composition similar to potassium feldspar, $KAlSi_3O_8$, crystallize in the hollandite structure type, while carnegieite, the Na aluminosilicate $NaAlSiO_4$, crystallizes in the Ca-ferrite structure type. Silicates with hollandite structure are considered as possible storage sites for alkaline cations in the mantle. An analog of sanidine, the potassium feldspar $KAlSi_3O_8$, with hollandite structure proved to be the second example (after stishovite) of a compound with silicon atoms in six-coordination and the third example (after garnet and perovskite) in which Si/Al isomorphism in the octahedrons was detected.
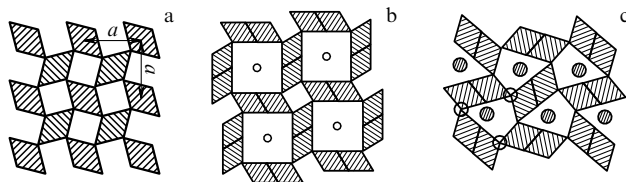

Figure 5. Octahedral frameworks in the structures of (a) rutile-stishovite, (b) hollandite, and (c) Ca-ferrite type.

The silicate phases that crystallize in the above structure types are of interest to geophysicists. Their interest in stishovite is also due to the discovery of stishovite in sedimentary rock dating back to the Palaeogene – Cretaceous boundary. This supports the hypothesis of a catastrophe resulting from the Earth's collision with an asteroid approximately 65 million years ago. The structure types of perovskite, its derivative K_2NiF_4, ilmenite, and pyrochlore are considered to be acceptable for silicates of the mantle.

The important role that silicates with Si octahedrons play in the lower mantle have determined the interest in the behavior at high pressures of their model analogs based on structural elements consisting of octahedrons. Bismutocolumbite, $Bi(Nb, Ta)O_4$, a mineral whose structure can be considered as an octahedral framework, belongs to such compounds. Single-crystal study of this mineral has shown that the Bi octahedron is the first to be distorted by high pressure [16], which leads to the rotational displacement of Nb octahedrons in the layers formed by them (Fig. 6). As a result of these changes, the structure loses its inversion center, and in this sense becomes an analog of stibiocolumbite. Thus, we can conclude that the stereoactivities of the lone electron pairs of the bismuth atoms at high pressures and of the Sb atoms under normal conditions are comparable.

Most silicates considered have been obtained at pressures above 20 GPa. At lower pressures (10 – 20 GPa) the silicates containing silicon in the four- and six-coordinations crystallize. These high-pressure phases, characteristic of the transition zone, include silicon-enriched varieties of garnet, pyroxene, and titanite and also two fairly abundant series of Mg-silicates and Na(K)-silicates. Many of these have germanate analogs, the so-called germanogermanates. In a book published in 1986 there is a chapter devoted to germanogermanates [17], where I predicted that such structures are acceptable for silicates of the deep geospheres. Today nearly
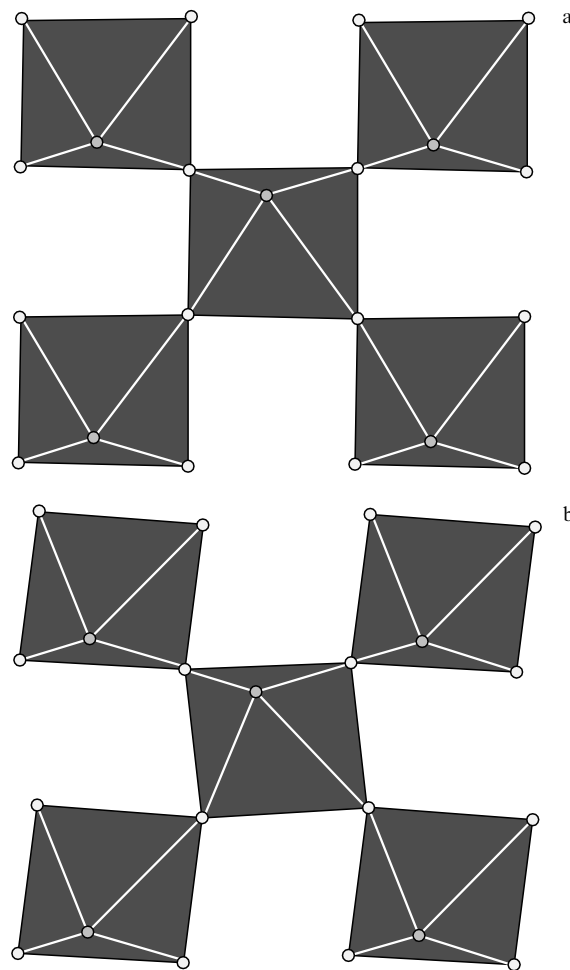

Figure 6. Distortion of the layer of (Nb, Ta) octahedrons in the structure of bismutocolumbite: (a) at atmospheric pressure, and (b) at 9.56 GPa.

10 out of the 16 types of germanogermanates have silicate analogs.

Among the mineral phases of this type I would like to mention compounds with structure types of the most important rock-forming minerals: garnet, sphene, and pyroxenes. The mineralogical importance of these compounds became especially evident after the discovery in 1970 of a silicon-enriched garnet, which became known as majorite, $(Mg, Na)_3(Fe, Al, Si)_2Si_3O_{12}$, and was found in the Coorara meteorite (Western Australia).

In addition to fairly simple structure types, characteristic of silicon-enriched garnets, pyroxenes, and titanite (sphene), the mineralogy of the transition zone has lately been supplemented with a new, exceptionally important and crystallochemically interesting series of Mg-silicates that contain (as the above phases) Si atoms in the four- and six-coordinations. It is assumed that at least a fraction of the water resources of the Earth is related to these minerals.

Topologically, the structures of this family of Mg-silicates are closely related to each other. Their study began with what became known as the anhydrous phase B, or $Mg_{14}^{[VI]}Si^{[IV]}Si_4O_{24}$. Clearly evident in the polyhedral framework of this structure are octahedral layers of brucite type, in which each eighth octahedron is vacant, while the occupied octahedrons contain regularly arranged Mg and
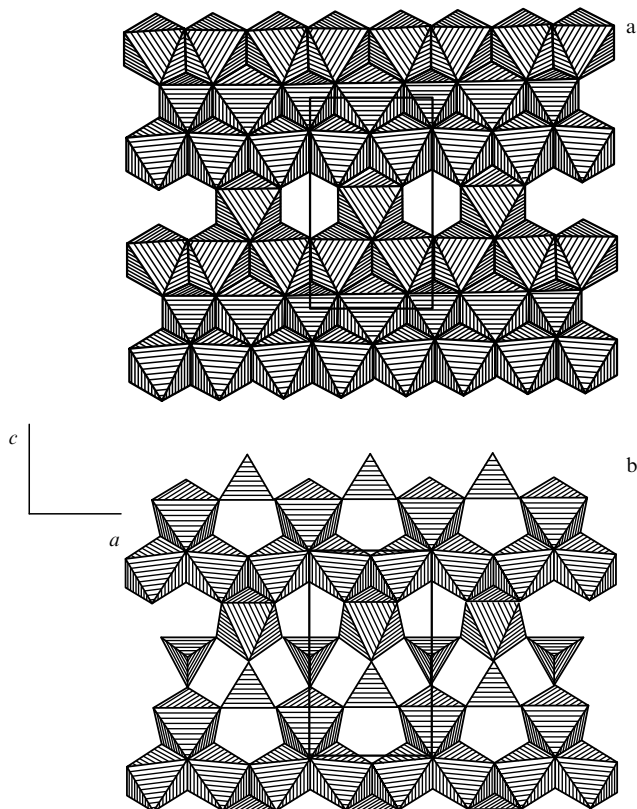
Figure 7. Structure of $Mg_{14}^{[VI]}Si^{[IV]}Si_4O_{24}$: (a) layer of regularly arranged MgO_6 and SiO_6 octahedrons, and (b) olivine-like layer (according to Ref. [18]).

Si atoms [18]. These octahedral layers alternate with pairs of layers of olivine type formed by Mg octahedrons and Si tetrahedrons (Fig. 7). Unlike this phase, in the structure of the other, hydrogenous, phase B of this family, $Mg_{12}^{[VI]}Si^{[IV]}Si_3O_{19}(OH)_2$, the mixed layer is similar to humite [18] (Fig. 8). Structurally coupled models have also been proposed for three chemically close phases of this series: the superhydrogenous phase B, $Mg_{10}Si_3O_{14}(OH)_4$, phase D, $MgSi_2H_2O_6$, and phase E, $Mg_{2.4}Si_{1.21}O_6H_{2.36}$.

Silicosilicates of alkaline cations contain silicon atoms in six-coordination and are much more open structures (compared to all those discussed above). Many such structures are analogs of germanogermanates synthesized earlier. Chiefly these are structures of alkaline silicates, analogs of wadeite, $K_2Si_4O_9$ and $Rb_2Si_4O_9$, whose mixed frameworks contain ternary rings of Si tetrahedrons coupled by isolated Si octahedrons.

A large group of alkaline silicates with Si tetrahedrons and Si octahedrons also have low-density mixed frameworks with highly diversified structural elements (see Table 1). In recent years their number has increased, and many of them have germanogermanate analogs.

In conclusion I would like to note that stishovite is the cornerstone of this entire group of silicate phases that may exist in the deep geospheres. Today it is clearly evident that the mantle mineralogy is not as primitive as it seemed not so long ago. I believe that in the years to come we will witness new discoveries in this elegant and enigmatic field of structural mineralogy.
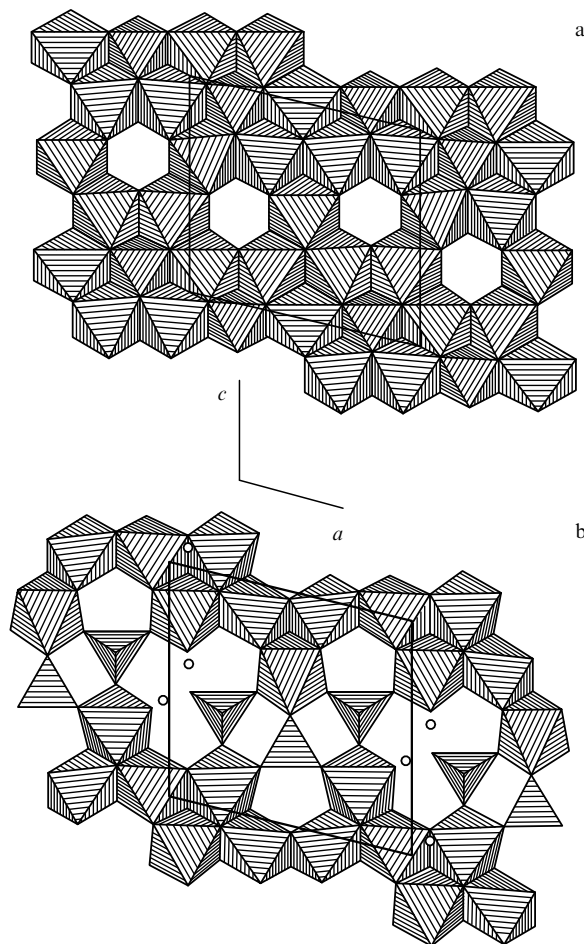

Figure 8. Structure of $Mg_{12}^{[VI]}Si^{[IV]}Si_3O_{19}(OH)_2$: (a) layer of regularly arranged MgO_6 and SiO_6 octahedrons, and (b) humite-like layer (according to Ref. [18]).

Table 1. Na-silicates synthesized under high pressures, and their structural characteristics.

Compound	Elements of mixed framework	Pressure of synthesis, GPa; references
$Na_2Si[Si_2O_7]$	Diorthogroups Si_2O_7, coupled by Si octahedrons	9; [19]
$Na_8Si[Si_6O_{18}]$	Sixfold rings of Si tetrahedrons coupled by Si octahedrons	9; [20]
$Na_6Si_3[Si_9O_{27}]$	Ninefold rings of Si tetrahedrons coupled by Si octahedrons	6; [21]
$Na_2CaSi[Si_5O_{14}]$	Layers of Si tetrahedrons coupled by Si octahedrons	8 – 16; [22]

References

1. Collerson K D et al. *Science* **288** 1215 (2000)
2. Pushcharovskiĭ Yu M, Pushcharovskiĭ D Yu *Geotektonika* **33** (1) 3 (1999) [*Geotectonics* **33** 1 (1999)]
3. Dubrovinsky L S et al. *Nature* **388** 362 (1997)

4. Knittle E, Jeanloz R *Geophys. Res. Lett.* **13** 1541 (1986)
5. Dubrovinsky L et al. *Nature* **412** 527 (2001)
6. Mazin I I et al. *Am. Mineral.* **83** 451 (1998)
7. Dubrovinsky L S et al. *Eur. J. Mineral.* **13** 857 (2001)
8. Pasternak M P et al. *Phys. Rev. Lett.* **79** 5046 (1997)
9. Funamori N, Jeanloz R *Science* **278** 1109 (1997)
10. Helffrich G R, Wood B J *Nature* **412** 501 (2001)
11. Finger L W, Hazen R M *Acta Crystallogr. B* **47** 561 (1991)
12. Scott H P, Williams Q, Knittle E *Phys. Rev. Lett.* **88** 015506 (2002)
13. Stishov S M, Popova S V *Geokhimiya* (10) 837 (1961) [*Geochem.* (10) 923 (1961)]
14. Hazen R, Finger L *Science* **201** 1122 (1978)
15. Fiquet G *Z. Kristallogr.* **216** 248 (2001)
16. Kazantsev S S et al., in *Tezisy III Nats. Konf. po Primeneniyu Rentgenovskogo, Sinkhrotronnogo Izlucheniĭ, Neĭtronov i Élektronov dlya Issledovaniya Materialov* (*RSNÉ*), *Moskva, 2001* (Abstracts of 3rd National Conference on the Use of X-ray and Synchrotron Radiations, Neutrons, and Electrons in the Studies of Materials (XSNE), Moscow 2001) (Moscow: Izd. Inst. Kristallografii Ross. Akad. Nauk, 2001) p. 83
17. Pushcharovskiĭ D Yu *Strukturnaya Mineralogiya Silikatov i ikh Sinteticheskikh Analogov* (Structural Mineralogy of Silicates and their Synthetic Analogs) (Moscow: Nedra, 1986)
18. Finger L W et al. *Nature* **341** 140 (1989)
19. Fleet M E, Henderson G S *Phys. Chem. Mineral.* **22** 383 (1995)
20. Fleet M E *Am. Mineral.* **83** 618 (1998)
21. Fleet M E *Am. Mineral.* **81** 1105 (1996)
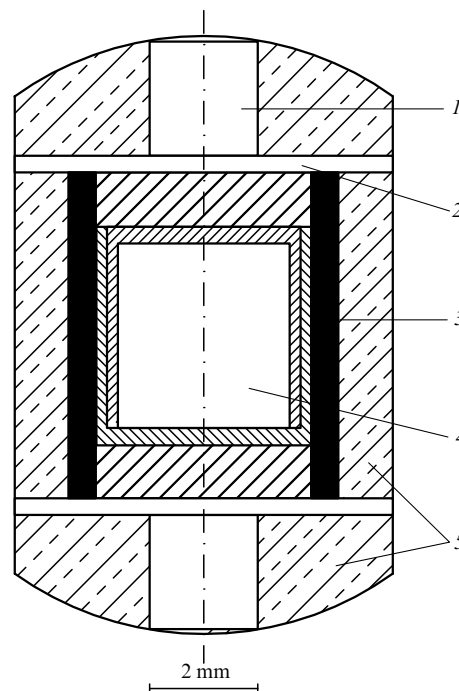22. Gasparik T et al. *Am. Mineral.* **80** 1269 (1995)

Hydrothermal growth of stishovite (SiO$_2$)

N A Bendeliani

1. Introduction

Single stishovite crystals have been grown by the hydrothermal method in the $SiO_2 - H_2O$ system under a pressure of 9 – 9.5 GPa in the 1170 – 770 K temperature interval. The method produced well-cut, transparent crystals of prismatic habit with the faces (110) and (111) and maximum dimensions of $500 \times 500 \times 2400$ μm.

The advances in growing and studying single stishovite crystals achieved during the last 40 years, starting with the discovery of this silica phase which plays an important role in geophysics and planetary sciences, have been limited to the results of three experiments [1 – 3]. Using accidentally grown single-crystal grains with sizes of 200 – 300 μm, the researchers were able to measure the refractive index and microhardness [1] and decipher the crystal structure [2]. Ramley et al. [3] studied the effects of hydrogen infusion into the lattice and observed acicular crystals that were up to 1000 μm long but only 25 μm wide. The ever growing interest in the properties of stishovite has led to the need for developing a fairly simple and reliable method of growing large and perfect single crystals of this phase. This problem has been solved at the Institute for High Pressure Physics of the Russian Academy of Sciences [4].

2. Experiment

Crystal growth was done in a Konak-type high-pressure cell with automatic monitoring of loading and programmed control of the current strength in the heater. The dependence of the temperature on the current strength was determined in a preliminary experiment. Figure 1 shows a schematic of the

Figure 1. Schematic of a high-pressure cell: *1*, input lead; *2*, metal disk; *3*, graphite heater; *4*, ampoule; *5*, container

high-pressure cell. The active volume of the hermetically sealed platinum ampoule was ~ 25 mm^3. The temperature gradient along the ampoule's height did not exceed 20 at 1200 K. The source materials were a powder of natural quartz with a grain size of 10 – 20 μm and distilled water. The amount of water was estimated by the ratio of the volumes of the components and ampoule.

3. Results and discussion

Using the example of coesite, a high-pressure phase of SiO$_2$ less dense than stishovite, Dyuzheva et al. [5] showed that the classical method of hydrothermal growth in modified form is realized fairly simply in conditions of extreme compression. Hence, provided that the necessary equipment is available, the solution of this problem is reduced primarily to determining the solubility of stishovite in an aqueous fluid.

The pressure of 9 – 9.5 GPa (the phase transition in Sn) under which the growing process took place proved to be sufficiently high for the system not to leave the stishovite regime in the course of the entire experiment (six to seven hours). The position of the liquidus on the (T, x) phase diagram under such pressure for a mixture consisting of the solution and stishovite was estimated by registering the sizes of stishovite grains in experiments with different component ratios in cooling from various temperatures. These data were then used to build the relevant part of the phase diagram (Fig. 2), which while being inaccurate in detail was quite sufficient for use as a working diagram. The melting temperature of ice-VII on the diagram has been taken from the paper by Pistorius et al. [6].

The best results were achieved with 6 mol.% of SiO$_2$ in the source mixture. The temperature was lowered from 1170 to 770 K with a cooling rate of roughly 1 K min^{-1}. Under such conditions the growth process produces transparent colorless, sometimes clear amber-coloured crystals of a prismatic habit with characteristic dimensions of $600 \times 600 \times 1200$ μm.